

Development of the Solid Oxide Fuel Cell

FRANCISCO JURADO

University of Jaén
Department of Electrical Engineering
Linares, Spain

JOSÉ R. SAENZ
LUIS FERNÁNDEZ

University of Cádiz
Department of Electrical Engineering
Cadiz, Spain

There are several types of fuel cells being developed for a variety of applications. The solid-oxide fuel cell is in an entirely solid state with no liquid components. This paper discusses the potential of a solid-oxide fuel cell fed by natural gas to serve locally as voltage support for the ac bus. A grid-connected fuel-cell plant consists of the fuel cell and the voltage-source inverter. The flux-vector control is used very effectively for the control of this inverter. Simulation results are presented to evaluate the performance of this fuel cell plant to alleviate voltage problems present on the ac grid.

Keywords fuel cells, power quality, inverter control

A solid-oxide fuel cell (SOFC) equipped with a pulsewidth modulation (PWM) inverter interface can be used to palliate power quality problems. The requirement is to have independent control over the real and reactive components of the power injected into the ac grid. Under these conditions, the distributed generator can be configured to behave as a dynamic voltage restorer (DVR). A series winding, associated with an inverter fed from the dc bus, can be included in the installation to inject the voltages required to support the ac grid voltage at the point of coupling during voltage sags and swells. These are mostly the result of single-phase faults on adjacent feeders.

Because the response time of the inverter is < 10 ms, it is not necessary to include its detailed model in the slow dynamic fuel cell system, except we can assume that power factor (PF) can be adjusted accordingly by the power conditioner.

However, what must be included in the model is the direct effect of this switching. In order to do so, the vector control strategy proposed in Chandorkar et al. (1993) has been simulated. It is a system that accepts commands in terms of real power, P , and reactive power, Q , and it executes them by means of several control loops.

Received 5 November 2002; accepted 27 December 2002.

Address correspondence to Francisco Jurado, University of Jaén, Department of Electrical Engineering, c/o Alfonso X N 28, Linares, Jaén 23 700, Spain. E-mail: fjurado@ujaen.es

Space-vector pulsewidth modulation (SVM) has recently become a very popular PWM method for voltage-fed converter ac machine drives because of its superior harmonic quality and extended linear range of operation. However, one difficulty of SVM is that it requires complex online computation that usually limits its operation up to several kilohertz of switching frequency. Of course, switching frequency can be extended by using a high-speed Digital Signal Processing (DSP) and simplified algorithms including lookup tables. Lookup tables, unless very large, tend to reduce pulsewidth resolution.

In this paper, the SVM have been implemented by neural networks (NNs). NNs, in general, are showing much promise for simplification of control and feedback signal processing (Kazmierkowski et al., 1995; Carrasco et al., 1997; Leyva et al., 1997).

This article is structured as follows. The next section presents a review of the fuel cell model. Then some basic concepts of the inverter control are presented. Next is a description of the architecture of NNs. The following section depicts some simulation results. Finally, conclusions are presented in the final section.

Fuel Cell Model

There are several types of fuel cells being developed for a variety of applications (Moore, 1997; *Scientific American*, 1999) and these have been extensively discussed in the literature. Unlike other variants, the SOFC is in an entirely solid state with no liquid components. Operation at elevated temperature is needed to achieve the necessary level of conductivity in the cell's solid electrolyte for it to operate efficiently. With an outlet temperature in the range of 900 to 1000°C, the efficiency of the cell alone is about 50%.

Typically the fuel cell system consists of SOFC generator modules in a parallel flow arrangement with the number of standard modules being determined by the plant power requirement. The SOFC generator module embodies a number of tubular cells, which are combined to form cell bundle rows, several of which are arranged side by side to make up the complete assembly.

The high efficiency of the system means that less carbon dioxide is generated than in contemporary power plants. In addition, the fuel is oxidized electrochemically without any interaction with atmospheric nitrogen so negligible amounts of nitrogen oxide are discharged to the environment.

Models for simulating fuel cell based plants have been developed (Bessette, 1994; Haynes, 1999; Padullés et al., 2000; Massardo and Lubelli, 2000; Campanari, 2001; Rao and Samuelsen, 2002). This paper provides a basic SOFC power section dynamic model used for performance analysis during normal operation. Some control strategies of the fuel cell system and response functions of the fuel processor and power section are combined to model the SOFC power generation system.

The chemical response in the fuel processor is usually slow as it is associated with the time to change the chemical reaction parameters after a change in the flow of reactants. This dynamic response function is modeled as a first-order transfer function with a 5 s time constant.

The electrical response time in the fuel cells is generally fast and mainly associated with the speed at which the chemical reaction is capable of restoring the charge that has been drained by the load. This dynamic response function is also modeled as a first-order transfer function but with a 0.8 s time constant.

Through the power conditioner, the fuel cell system can output not only real power but also reactive power. Usually, PF can be in the range of 0.8 to 1.0. The SOFC system dynamic model is given in Figure 1.

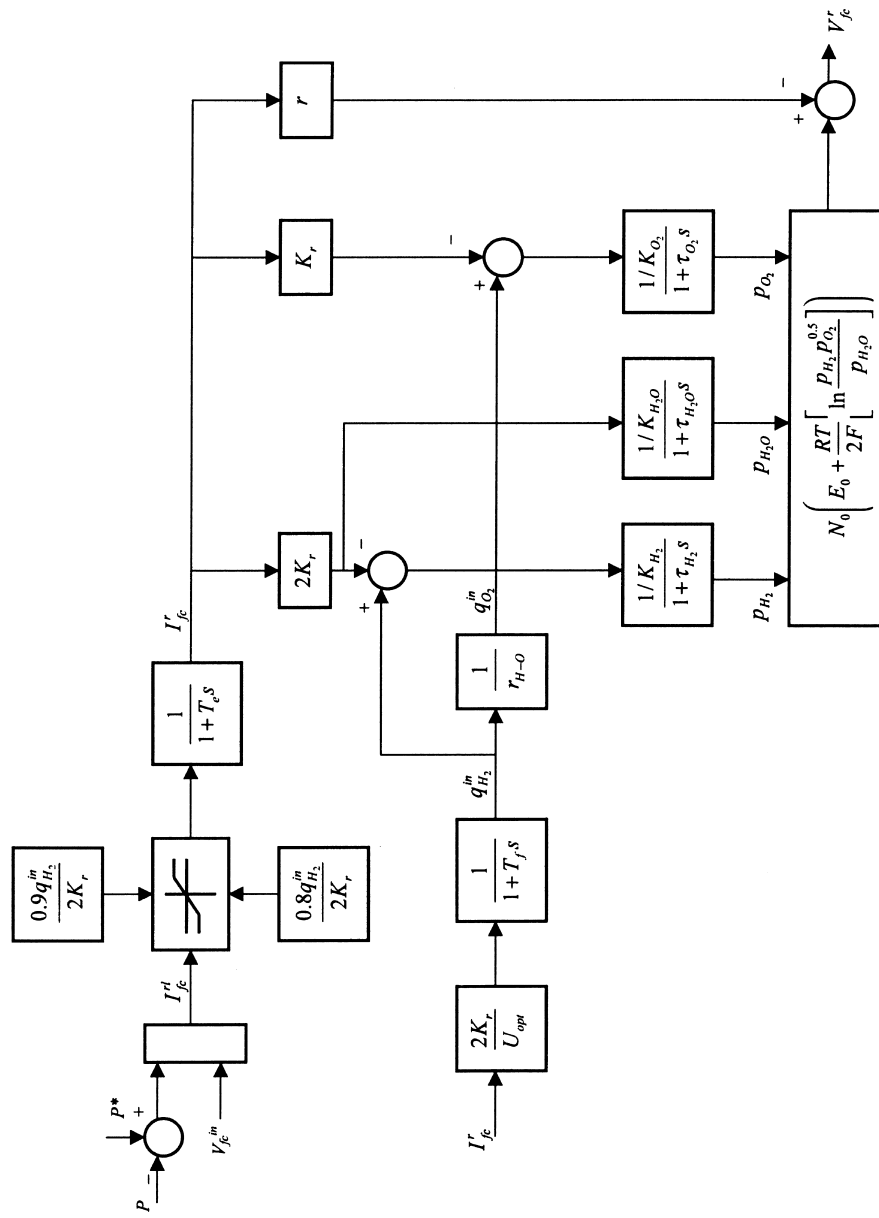


Figure 1. SOFC system dynamic model.

Utility-Connected Inverter Control

Essentially, inverter flux-vector control involves appropriately choosing the inverter voltage vectors so as to make the flux follow a reference flux vector within a specified tolerance band.

Because the modulator does not directly control the load, the response of the load quantities is not as fast. However, the advantage here is that it does lead to a general-purpose modulator whose task is to control the inverter flux vector to whatever value is specified by the outer control loop. The outer control loop can then be designed independently to generate the inverter flux-vector set point for achieving the desired final result.

Inverter flux-vector control can be used very effectively for the control of inverters that have their outputs connected to the main utility system. This section describes the flux control of a 3 phase inverter connected to the utility system through a sine-wave output filter. The control system for the inverter is given in Figure 2.

The instantaneous *position* of the rotating q - d reference frame axes is determined relative to the utility mains voltage, either by the use of a phase-locked loop (PLL) or by the use of a power-frequency droop characteristic as in Chandorkar et al. (1993). In either case, in the steady state the q - d frame angular frequency equals the mains frequency, and its position relative to the mains voltage determines the sharing of the total load power between the inverter and the utility mains.

The inverter controller is required to align the filtered output voltage vector, \mathbf{E} , with the rotating, q , axis of the reference frame. The inverter flux vector, ψ_v , can be used as a very effective forcing quantity to achieve this.

Further, being a continuous quantity, it is very convenient to use the flux vector to define the power angle, which essentially determines the flow of real power from the inverter to the load bus. In Figure 3, this is the angle between the vectors ψ_v and ψ_e , where ψ_e is the flux vector associated with the load bus voltage \mathbf{E} .

The inverter flux vector, ψ_v , is the forcing quantity used to align the filtered voltage vector with the rotating axis and to ensure that it has the desired magnitude.

To force the filtered voltage vector, \mathbf{E} , to assume the desired value, \mathbf{E}^* , the inverter flux-vector reference ψ_v^* can be generated by a proportional-integral (PI) controller acting on the voltage vector error, $\varepsilon = \mathbf{E}^* - \mathbf{E}$, in the rotating reference frame

$$\psi_v^* = k_p \varepsilon + k_i \int \varepsilon dt. \quad (1)$$

In this equation, the complex constants k_p and k_i are the gains of the rotating frame vector PI controller.

For the purpose of controller design, it is assumed that the inverter, as controlled by the flux modulator, is capable of producing the commanded flux vector at its output with negligible delay. That is, the assumption that $\psi_v = \psi_v^*$ is always valid.

Neural Networks

The PWM controller receives the ψ_v^* and δ_p^* signals at the input and translates to gate drive signals for the Insulated Gate Bipolar Transistors (IGBT) inverter. The terminal voltages and currents are sensed and filtered by low-pass filters. Figure 4 shows the topology of the NN-based SVM. It receives the ψ_v^* and δ_p^* signals at the input and generates symmetrical pulses for 3 phases at the output, as shown in Figure 4.

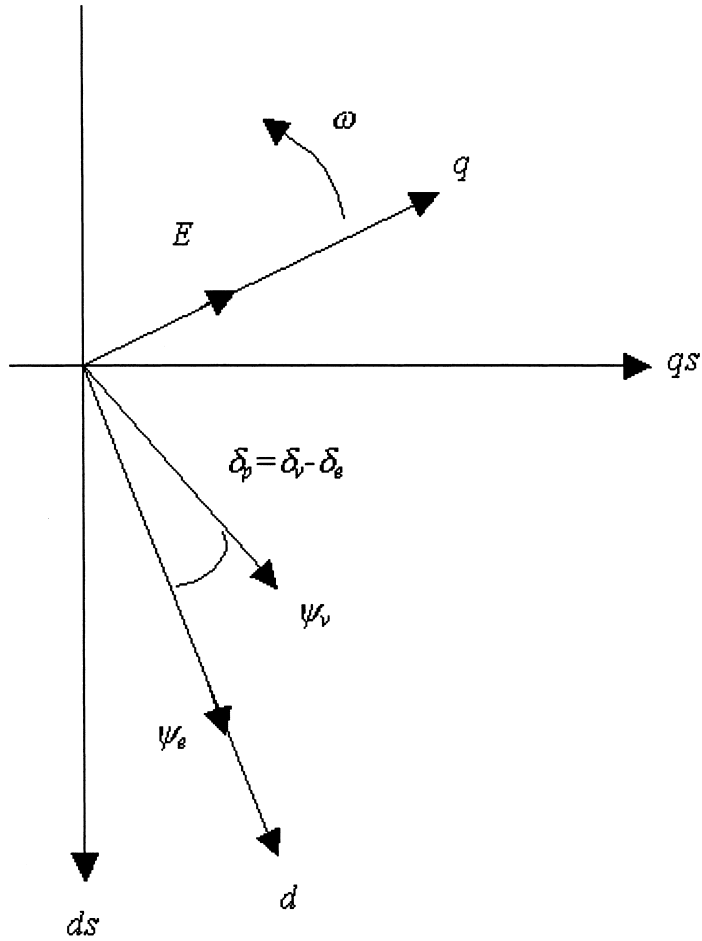


Figure 3. Flux-vector diagram of inverter.

Basically, the network consists of 2 subnets: the magnitude subnet (shown in the upper part), which implements the function $f(\psi_v^*)$ that is linear in the undermodulation region but nonlinear in the overmodulation region; and the angle subnet implements the pulsewidth function $g(\alpha^*)$ for the 3 phases at phase shift angles of $2\pi/3$ (Pinto et al., 2000; Pinto et al., 2001). Note that the sigmoidal activation functions of the angle subnet generate only unipolar outputs, and these are converted to bipolar outputs by adding a fixed bias in the denormalization process. The digital words corresponding to turn-on time (T_{ON}) of phase A can be expressed as

$$T_{A-ON} = f(\psi_v^*)g_A(\alpha^*) + \frac{T_S}{4}, \quad (2)$$

where T_S is the sampling time ($T_S = 1/f_{S\omega}$, $f_{S\omega}$ is the switching frequency), $g(\alpha^*)$ is the pulsewidth function of a phase at unit voltage amplitude, and $f(\psi_v^*)$ is the voltage magnitude function. For the symmetrical pulsewidth of each phase, the turn-off time can be given in the form

$$T_{OFF} = T_s - T_{ON}. \quad (3)$$

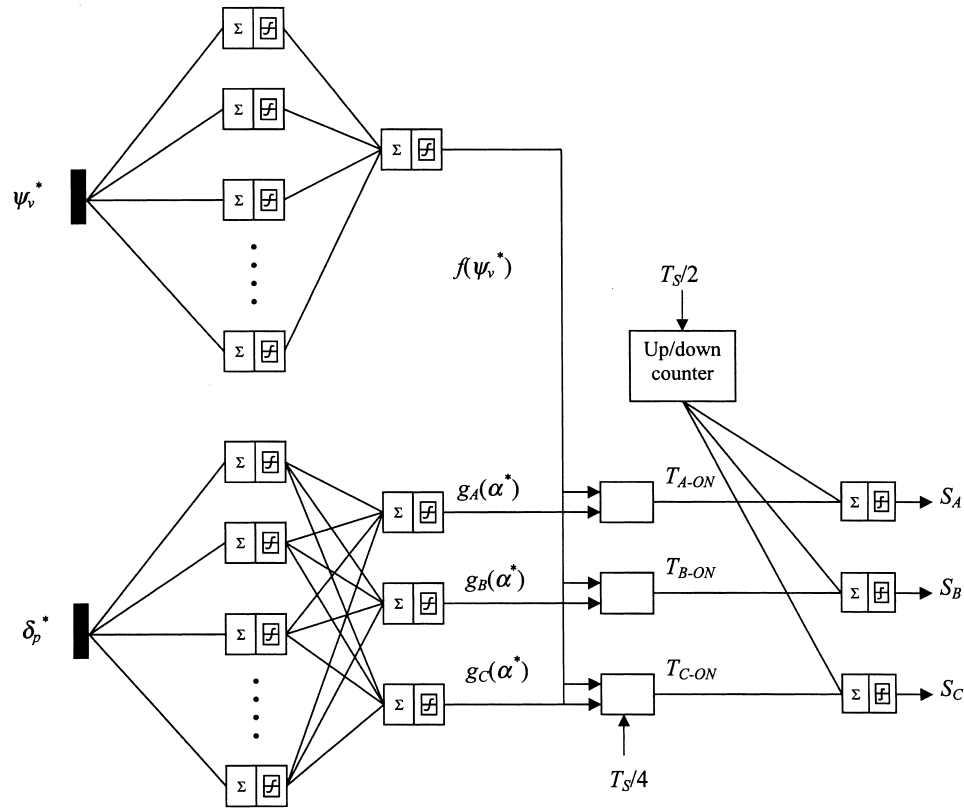


Figure 4. Topology of NN-based SVM modulator.

The training data were generated by simulation of a conventional SVM algorithm, and then a backpropagation technique in the MATLAB-based Neural Network Toolbox (MATLAB, 2000) was used for offline training. In the ANN-based SVM technique, the digital words corresponding to turn-on time are generated by the network and then converted to pulsewidths by a single timer.

Results

Figure 5 shows the test system used to carry out the various simulations. The majority of data for the fuel cell model has been extracted from Kuipers (1998), Singhal (1999), and a commercial leaflet describing a SOFC 100 kW plant.

The total simulation period is 0.5 s. Using the facilities available in MATLAB, the fuel cell plant is simulated to be in operation, as is expected to be the case in a practical situation. The results for the simulations are shown in Figures 6–11.

In each figure, the first simulation contains no fuel cell plant and the second simulation is carried out using the same scenario as above, but now with the fuel cell plant in operation

Different transformer winding connections between the fault location and load terminal will cause different sags at the load terminal due to imbalanced faults. Transformers with winding connections of Δ/Y , Y/Δ will result in the same sag at the load terminal. This consists of a large voltage drop on 2 phases and a relatively small drop on the third phase.

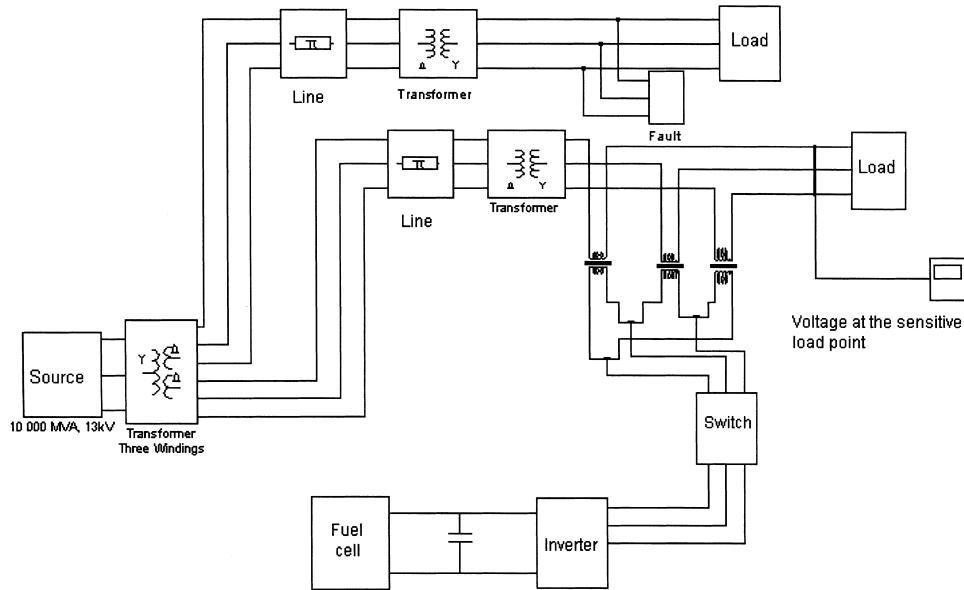


Figure 5. Test system implemented in MATLAB to carry out the simulations.

The transformer winding connections between the point of the fault and the equipment terminals swap the 3 phase voltages in case of an imbalanced sag.

Most of the faults on the utility transmission and distribution systems are single line-to-ground faults (SLGFs). An SLGF on the primary side of a Δ/Y or Y/Δ transformer will change into a phase-to-phase fault on the secondary side (Bollen, 1999). Figure 6 shows the phase voltage at the sensitive load point due to an SLGF of 18 cycles on phase A.

Line-to-line faults (LLFs) on the primary side of the transformer cause similar types of sag as SLGFs, but with lower voltage magnitude at the load terminal.

One of the phase voltages drops almost to zero, while the other 2 phase voltages drop to around 60% of the pre-fault voltage, as shown in Figures 7 and 8. The fault is placed between lines B and C.

Figure 9 depicts the voltage sag on phase A at the sensitive load point in Figure 5 due to a 3 phase fault of 300 ms duration. The voltage sag at the load point is 50% with respect to the reference voltage.

Figure 10 shows the voltage sag on phase A in Figure 5 due to a 3 phase fault of 200 ms duration and an induction motors percentage of 60%. Figure 11 depicts the voltage sag and induction motors percentage of 65%. These figures show the influence of induction motors on the shape and the duration of voltage sags.

Since it is a balanced fault, voltages in 3 phases are therefore the same, and phases B and C are not shown here. The voltage sag consists of a severe during-fault sag, directly due to the fault, and a less severe post-fault sag with longer duration, due to the induction motor reacceleration. The during-fault sag decays to zero in a few cycles.

An induction motor generally slows down, with energy being returned to the supply under generator action, during a fault. It simply operates as a generator for a short period and causes a decrease in sag. However, its reacceleration after fault clearance results in an extended post-fault (Bollen, 1995).

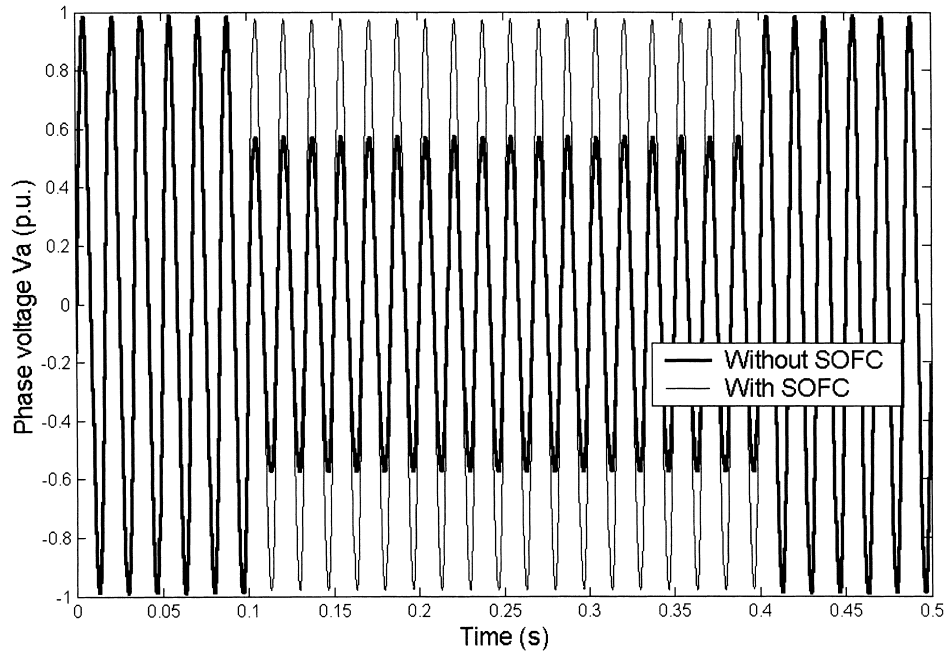


Figure 6. Phase voltage at the sensitive load point in Figure 5 due to an SLGF.

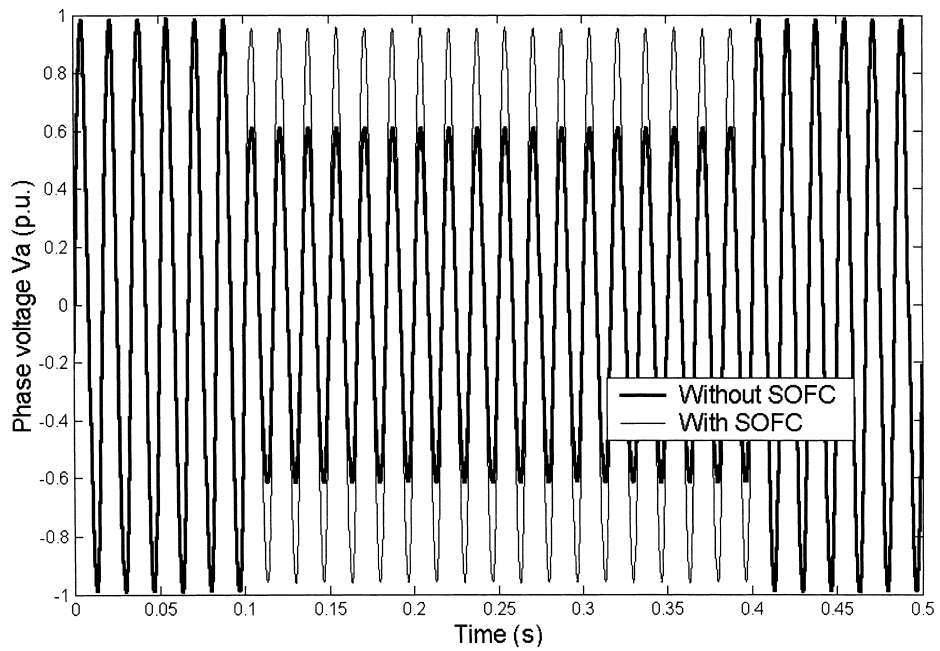


Figure 7. Phase voltage at the sensitive load point in Figure 5 due to an LLF on phase A.

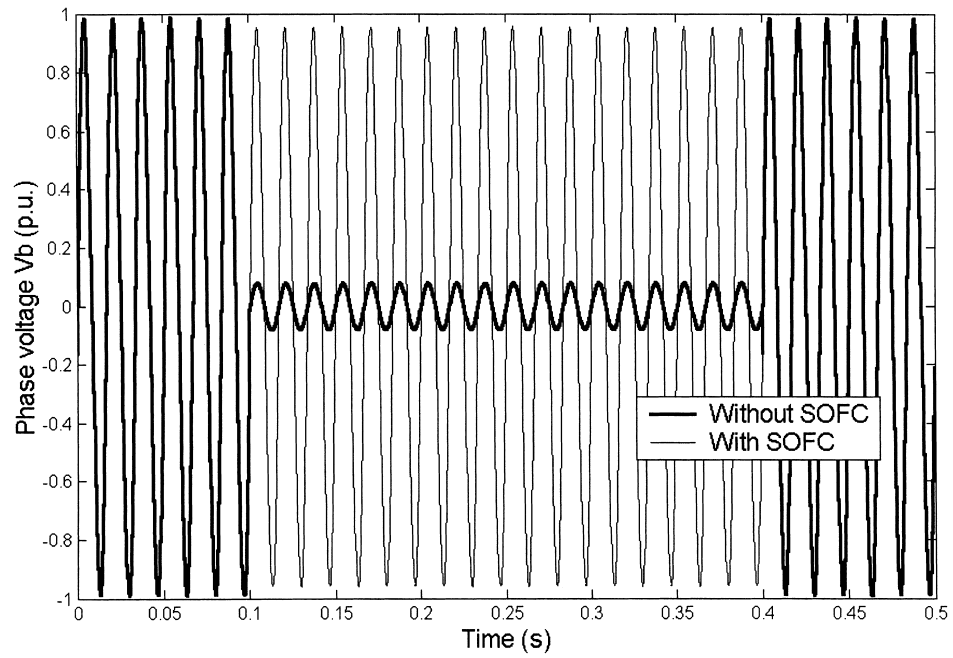


Figure 8. Phase voltage at the sensitive load point in Figure 5 due to an LLF on phase B.

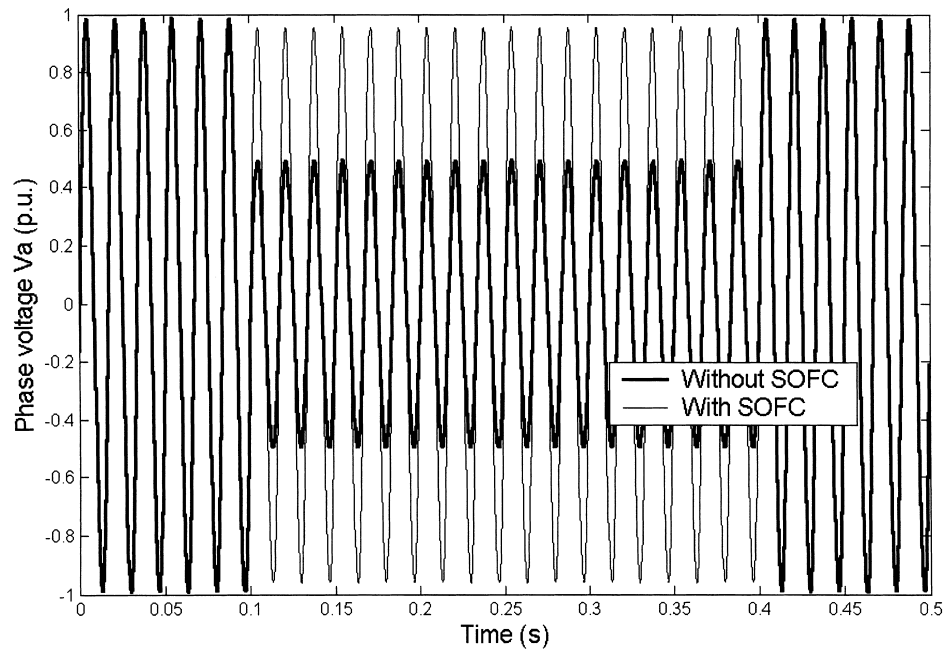


Figure 9. Phase voltage at the sensitive load point in Figure 5 due to a 3 phase fault.

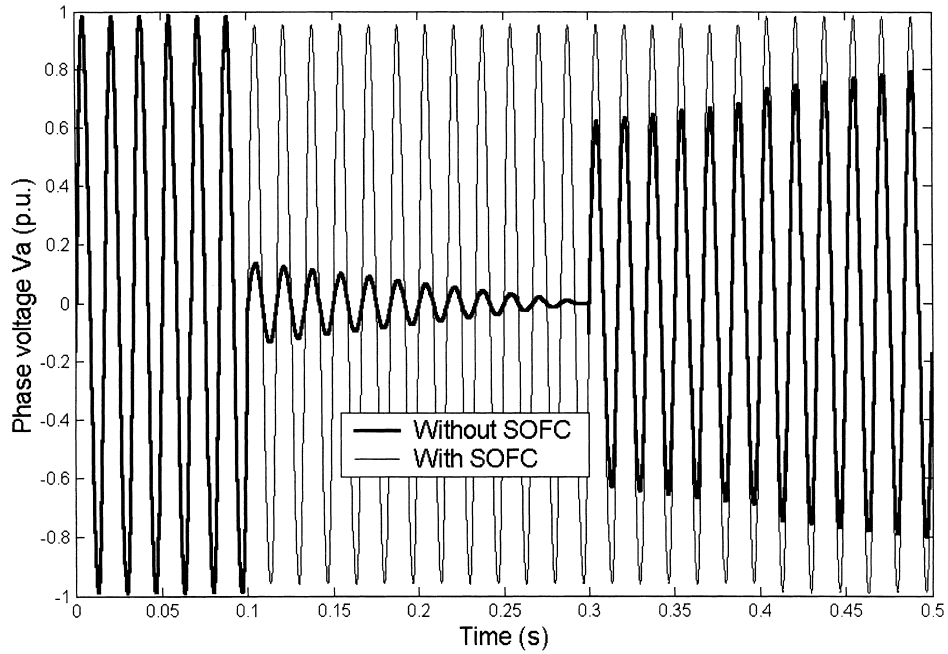


Figure 10. Phase voltage at the sensitive load point in Figure 5 due to a 3 phase fault. Induction motors percentage of 60%.

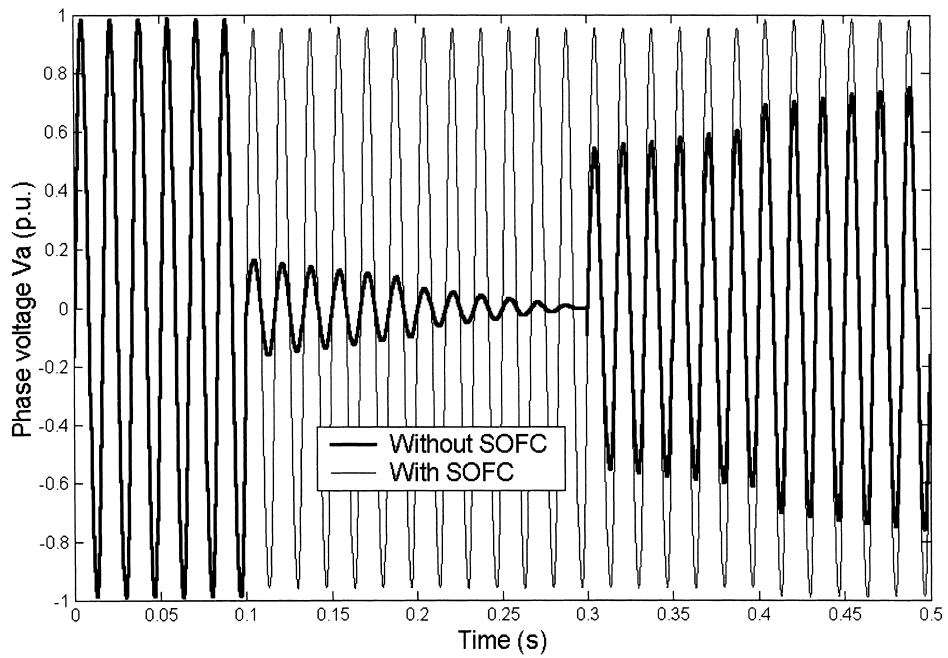


Figure 11. Phase voltage at the sensitive load point in Figure 5 due to a 3 phase fault. Induction motors percentage of 65%.

Conclusions

This paper discusses the potential of fuel cell plants for enhancement of power quality. In particular, fuel cell plants can serve locally as voltage support of the ac bus.

Voltage sag is a significant disturbance that may lead to tripping and high cost to sensitive customers. When the fuel cell plant is in operation, the voltage sag is mitigated almost completely and the voltage at the sensitive load point is maintained, as demonstrated by the examples given in this paper.

References

- Bessette, N. F. 1994. *Modeling and Simulation for Solid Oxide Fuel Cell Power Systems*, Ph.D. thesis. Georgia Institute of Technology.
- Bollen, M. 1995. The influence of motor reacceleration on voltage sags. *IEEE Trans. Ind. Applicat.* 31(4):667–674.
- Bollen, M. 1999. *Understanding Power Quality Problems. Voltage Sags and Interruption*. Piscataway, NJ: IEEE Press.
- Campanari, S. 2001. Thermodynamic model and parametric analysis of a tubular SOFC module. *Journal of Power Sources* 92(1–2):26–34.
- Carrasco, J. M., J. M. Quero, F. P. Ridaio, M. A. Perales, and L. G. Franquelo. 1997. Sliding mode control of a DC/DC PWM converter with PFC implemented by neural networks. *IEEE Trans. Circuits and Systems I* 44(8):743–749.
- Chandorkar, M. C., D. M. Divan, and R. Adapa. 1993. Control of parallel connected inverters in stand-alone AC supply systems. *IEEE Trans. Ind. Applicat.* 29(1):136–143.
- Haynes, C. L. 1999. *Simulation of Tubular Solid Oxide Fuel Cell Behavior for Integration Into Gas Turbine Cycles*, Ph.D. thesis. Georgia Institute of Technology, Atlanta, Georgia, USA.
- Kazmierkowi, M. P., D. L. Sobczuk, and M. A. Dzlaniakowski. 1995. Neural network current control of VS-PWM inverters. *Proc. of EPE Conference* 1415–1420.
- Kuipers, J. A. 1998. Proceedings of the Fuel Cell Seminar.
- Leyva, R., L. Martinez-Salamero, B. Jammes, J. C. Marpinard, and F. Guinjoan. 1997. Identification and control of power converters by means of neural networks. *IEEE Trans. Circuits and Systems I* 44(8):735–742.
- Massardo, A. F., and F. Lubelli. 2000. Internal reforming solid oxide fuel cell-gas turbine combined cycles (IRSOFC-GT): Part A-Cell model and cycle thermodynamic analysis. *J. Eng. Gas Turbines and Power* 122(27):27–35.
- MATLAB. 2000. *Neural Network Toolbox User's Guide with MATLAB*, Version 4. Natick, MA: The Math Works Inc.
- Moore, T. 1997. Market potential high for fuel cells. *EPRI Journal* 22(3):6–17.
- Padullés, J., G. W. Ault, and J. R. McDonald. 2000. An integrated SOFC plant dynamic model for power systems simulation. *Journal of Power Sources* 86(1–2):495–500.
- Pinto, J. O. P., B. K. Bose, L. E. Borges, and M. P. Kazmierkowski. 2000. A neural network based space vector PWM controller for voltage-fed in-verter induction motor drive. *IEEE Trans. Ind. Applicat.* 36(6):1628–1636.
- Pinto, J. O. P., B. K. Bose, and L. E. B. da Silva. 2001. A stator flux oriented vector-controlled induction motor drive with space vector PWM and flux vector synthesis by neural networks. *IEEE Trans. Ind. Applicat.* 37(5):1308–1318.
- Rao, A. D., and G. S. Samuelsen. 2002. Analysis strategies for tubular solid oxide fuel cell based hybrid systems. *J. Eng. Gas Turbines and Power* 124(3):503–509.
- Scientific American*. 1999. The future of fuel cells, pp. 72–83.
- Singhal, S. C. 1999. Progress in tubular solid oxide fuel cell technology. *Proc. Solid Oxide Fuel Cells*. Honolulu, HI, Oct. 17–22; 39–51.
- Singhal, S. C. 1997. *Electrochemical Proceedings* 37:97–18.